

Non-equilibrium quantum transport theory: current and gain in quantum cascade lasers

Tillmann Kubis · Catherine Yeh · Peter Vogl

Published online: 12 December 2007
© Springer Science+Business Media LLC 2007

Abstract We have developed a self-consistent non-equilibrium Green's function theory (NEGF) for charge transport and optical gain in THz quantum cascade lasers (QCL) and present quantitative results for the I - V characteristics, optical gain, as well as the temperature dependence of the current density for a concrete GaAs/Al₁₅Ga₈₅As QCL structure. Phonon scattering, impurity, Hartree electron-electron and interface roughness scattering within the self-consistent Born approximation are taken into account. We show that the characteristic QCL device properties can be successfully modeled by taking into account a single period of the structure, provided the system is consistently treated as open quantum system. In order to support this finding, we have developed two different numerically efficient contact models and compare single-period results with a quasi-periodic NEGF calculation. Both approaches show good agreement with experiment as well as with one another.

Keywords Quantum cascade lasers · QCL · Quantum transport · NEGF

1 Introduction

A realistic description of carrier transport in open multi-quantum-well devices such as cascade lasers (QCL) is a challenging task, since carrier confinement, quantum interference effects, as well as incoherent scattering compete with one another on an equal scale.

It is well established that the non-equilibrium Green's function theory (NEGF) is the most general scheme for the prediction of incoherent quantum transport [1–3]. It allows for the calculation of scattering states (represented by the retarded electron Green's function G^R) and their non-equilibrium occupation (represented by the lesser Green's function $G^<$) in a self-consistent manner.

A realistic QCL structure consists of a large number of periodically repeated multi-quantum-well structures that are coupled to leads. A fully quantum mechanical transport calculation through such an extended device is numerically unfeasible. Therefore, one needs to develop contact models that faithfully reproduce the intrinsic transport properties of the active region of QCLs while simultaneously limiting the simulation region to effectively one or a few periods.

In semiclassical QCL simulations [4], this problem has been tackled by implementing periodic boundary conditions where electrons that leave the device on the drain side are reinjected on the source side. In the framework of NEGF, Lee and Wacker [2] have developed an analogous scheme in a Wannier basis that mimics this quasi-periodic nature of QCLs by explicitly assuming periodic conditions for all Green's functions. This approach is physically very appealing but requires simplifying approximations both in the number of basis states as well as in the scattering self energies to remain numerically feasible.

In this paper, we have attempted to implement the NEGF formalism in a real space basis very accurately [5] but de-

T. Kubis (✉) · P. Vogl
Walter Schottky Institute, TU München, Am Coulombwall 3,
85748 Garching, Germany
e-mail: kubis@wsi.tum.de

P. Vogl
e-mail: vogl@wsi.tum.de

C. Yeh
University of California, Santa Barbara, CA 93106, USA

veloped two complementary approximate schemes to model the open boundary conditions for QCLs. As we will show, both of these schemes yield similar results that suggest that the present calculations provide valid insight into the complex phenomena that govern the carrier dynamics and optics in QCLs. In addition, we have studied the influence of temperature on the characteristic properties of QCLs.

2 Method

All quantum cascade structures in this paper are GaAs/AlGaAs quantum well heterostructures that are homogeneous in the lateral x, y directions. They are assumed to be in contact with two equilibrium reservoirs at $z = 0$ and $z = L$, respectively. The electrons are described within a one-band model with a variable energy dependent (nonparabolic) effective mass $m^*(z, E)$.

The NEGF method requires the solution of four coupled partial differential equations. These equations read, in operator form,

$$\begin{aligned} (E - H_0 - e\Phi - \Sigma^R)G^R &= 1, \\ G^< &= G^R \Sigma^< G^{R\dagger}, \\ \Sigma^< &= G^< D^<, \quad \Sigma^R = G^R D^R + G^R D^< + G^< D^R, \end{aligned} \tag{1}$$

where H_0 is the single-electron Hamiltonian, Φ is the electrostatic potential, D is the sum of all environmental Green's functions, and Σ denotes the self-energy. We have implemented these expressions in a real space basis so that, e.g., the self-energies $\Sigma(z, z', k_{\parallel}, E)$ are functions of two spatial coordinates, the lateral momentum, and the energy. In this way, the scattering states, the transition probabilities between them and their occupations are calculated self-consistently. An important role of this self-consistency is to ensure that the total scattering probability into each final state never exceeds the Pauli blocking limit [5]. Once the Green's functions have been calculated, observables such as the absorption coefficient, the current and the electron density can be calculated straightforwardly [1–3]. Numerical details have been given in [5] and will be discussed extensively in a forthcoming publication.

We take into account inelastic acoustic and polar-optical phonon scattering, scattering by charged impurities, interface roughness, and by electron-electron interaction in the Hartree approximation. The full nonlocal momentum and energy dependence of the phonon, impurity and interface roughness self-energies are taken into account. We employ the self-consistent Born approximation in calculating G^R and $G^<$ which is a prerequisite for guaranteeing current conservation in this formalism.

The spatial dependence of the electrostatic potential is uniquely determined by 3 conditions: (i) global charge neutrality of the device, (ii) the potential drop in the device

equals the difference in the chemical potentials of the contacts, (iii) an equilibrium Fermi distribution in the leads. In order to avoid reflections, interferences, and charge oscillations at the contacts, we extend the density of states adjacent to the leads continuously into the leads. This implies that we also include scattering within the leads. This scheme is analogous to the one proposed by [6], but we maintain the full off-diagonal character of the self energies. Fortunately, the high barriers within a QCL cause the current to be insensitive to the scattering self-energies within the leads.

We have modeled the open boundary conditions for QCLs in two ways. First, we have considered a single active zone as the device region and attached source and drain leads with equilibrium Fermi distributions to the left and right hand side of the device, respectively. Secondly, we have effectively calculated two QCL periods by treating the second period as being part of the field-free source and drain lead. As will be explained in more detail below, this mimics the quasi-periodic nature of QCL structures.

3 Results

We have applied this formalism to carrier transport and optical gain within the active region of the THz GaAs/Al_{0.15}Ga_{0.85}As QCL structure of [7]. The geometry of this structure can be symbolically denoted by (30) 92 (55) 80 (27) 66 (41) 155. All quantities are given in Å, the values in parentheses indicate Al_{0.15}Ga_{0.85}As barrier widths, and the underlined value indicates an n -doped well with $n = 1.25 \times 10^{16} \text{ cm}^{-3}$.

The interface roughness is described by an autocorrelation length L_a and a variable step height δz [3, 8, 9]. We have used the values $L_a = 8 \text{ nm}$ and $\delta z = 0.6 \text{ nm}$ [10]. The electron-phonon and impurity interaction parameters have been taken from [11].

We now discuss the presently developed lead models in more detail. Figs. 1(a) and (b) depict the conduction band profile (full lines) within the device as well as within a portion of the semi-infinite leads (grey-shaded regions). In the case depicted in Fig. 1(a), we attach two homogeneously n -doped semi-infinite GaAs leads with $n = 1.25 \times 10^{16} \text{ cm}^{-3}$ to a single period of the active region of the QCL. We term this model the single-period case. In Fig. 1(b), we show an alternative approach that we term quasi-periodic case. Apart from being field-free, each of the two lead regions is an exact repetition of the appropriate half of the active zone and thus repeats the density of states and doping concentration of the active region. We find the potential profile deeper within the contacts to have negligible influence on the device characteristics. In this way, we mimic periodic boundary conditions.

In Fig. 2, we compare experiment with these two complementary contact models. Both types of NEGF calculations reproduce the experimental current nicely up to 60 mV

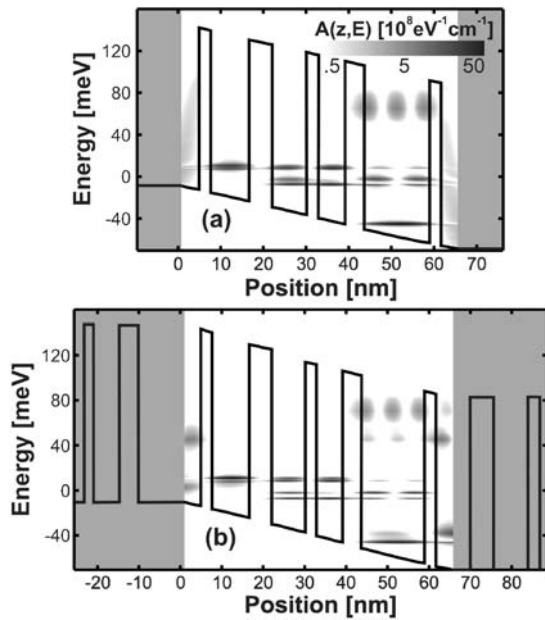


Fig. 1 Contour plots of the energy resolved spectral function of the QCL of [7] as a function of position z and energy. The *solid lines* indicate the conduction band at the bias voltage of 60 mV. (a) Single period contact model. (b) Quasi-periodic contact model

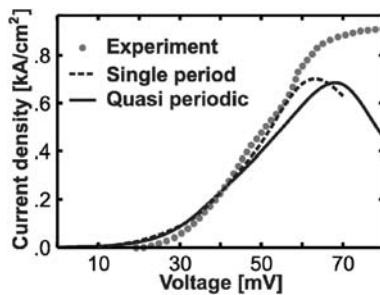


Fig. 2 I - V curve of the active region of the QCL in Fig. 1 at 40 K. Comparison between the NEGF calculations based on the single-period contact model (*dashed*), the quasi-periodic contact model (*full line*) and the experimental results of [7] (*grey dots*)

where the calculated gain reaches its maximum. For higher voltages, the electronic states that feed the occupation inversion become misaligned which decreases the current and yields a negative differential resistivity. In experiment, however, hot electrons cause a continuous increase of the current.

To get more insight into the difference between the two contact models, Figs. 1(a) and (b) show a contour plot of the energy resolved and spatially resolved spectral density $A(z, E) = i[G^R(z, z, 0, E) - G^{R\dagger}(z, z, 0, E)]$ for vanishing lateral momentum $k_{\parallel} = 0$ and a bias voltage of 60 mV. The zero in energy marks the chemical potential in the left contact. The maxima of the spectral function represent resonances. Their finite width is partly caused by the incoherent scattering mechanisms. In Fig. 1(a), the large continu-

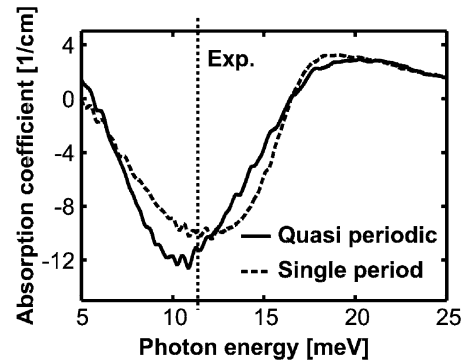


Fig. 3 Absorption coefficient of the QCL in Fig. 1 at the center of the active region ($z = 30$ nm) as a function of photon energy. *Dashed line*: single period contact model. *Solid line*: quasi-periodic contact model. The maximum of the experimental emission photon energy is indicated by the *dotted line*

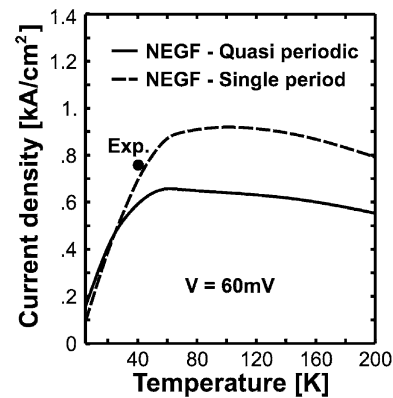


Fig. 4 Current density of the QCL in Fig. 1 for the two contact models (*dashed line*: single period, *full line*: quasi-periodic) as a function of temperature. The bias voltage is set to 60 mV. The *dot* marks the experimental current density [7] at approximately 40 K

ous spectral function near the lead/device boundary represents the continuous bulk-like density of states in the leads. By contrast, the spectral function in Fig. 1(b) shows two broad resonances that are caused by the tunneling processes through the confining potentials inside the leads. In spite of these drastic differences in the lead density of states of the two models, the spectral function in the interior of the device is very similar. More importantly, both models yield a calculated gain that peaks very closely to the experimental emission line at 2.75 THz (11.4 meV), as shown in Fig. 3. An extensive discussion of the physics controlling this optical gain is given in [12].

It is known experimentally [13] that the temperature inside a QCL raises with electrical power. It is therefore interesting to calculate the current as a function of the temperature T that influences the phonon population and the lead carrier distribution. The predictions for the two contact models are shown in Fig. 4 and compared to an experimental value at approximately 40 K [7]. The behavior of the current

as a function of T reflects the resonant tunneling process. For the given bias, only few electrons can resonantly tunnel through the QCL. A higher temperature smears out the distribution so that more electrons can match the resonance condition. If we increase the temperature further, however, a large portion of the electrons is spread out energetically and lies predominantly off-resonance. The fact that the current is smaller for the quasi-periodic contact model stems from the smaller density of states. In conclusion, both contact models yield good agreement with experiment.

Acknowledgements The authors acknowledge financial support from the Deutsche Forschungsgemeinschaft (SFB 631), the Österreichische Fonds zur Förderung der Wissenschaft (SFB IRON), the Nano Initiative Munich, and the Fulbright Commission.

References

1. Wacker, A.: Gain in quantum cascade lasers and superlattices: a quantum transport theory. *Phys. Rev. B* **66**, 085326 (2002)
2. Lee, S.-C., Wacker, A.: Nonequilibrium Green's function theory for transport and gain properties of quantum cascade structures. *Phys. Rev. B* **66**, 245314 (2002)
3. Lake, R., Klimeck, G., Bowen, R., Jovanovic, D.: Single and multiband modeling of quantum electron transport through layered semiconductor devices. *J. Appl. Phys.* **81**, 7845 (1997)
4. Iotti, R.C., Rossi, F.: Microscopic modeling of semiconductor-based quantum devices: a predictive simulation strategy. *Phys. Stat. Sol. (B)* **238**, 462 (2003)
5. Kubis, T., Vogl, P.: Self-consistent quantum transport theory: applications and assessment of approximate models. *J. Comput. Electron.* **6**, 183 (2007)
6. Svizhenko, A., Anantram, M.P.: Effect of scattering and contacts on current and electrostatics in carbon nanotubes. *Phys. Rev. B* **72**, 085430 (2005)
7. Benz, A., Fasching, G., Andrews, A.M., Martl, M., Unterrainer, K., Roch, T., Schrenk, W., Golka, S., Strasser, G.: Influence of doping on the performance of terahertz quantum-cascade lasers. *Appl. Phys. Lett.* **90**, 101107 (2007)
8. Nag, B.R.: Interface roughness scattering limited mobility in AlAs/GaAs, Al_{1.3}Ga_{0.7}As/GaAs and Ga_{0.5}In_{0.5}P/GaAs quantum wells. *Semicond. Sci. Technol.* **19**, 162 (2004)
9. Unuma, T., Yoshita, M., Noda, T., Sakaki, H., Akiyama, H.: Intersubband absorption linewidth in GaAs quantum wells due to scattering by interface roughness, phonons, alloy disorder, and impurities. *J. Appl. Phys.* **93**, 1586 (2003)
10. Leosson, K., Jensen, J.R., Langbein, W., Hvam, J.M.: Exciton localization and interface roughness in growth-interrupted GaAs/AlAs quantum wells. *Phys. Rev. B* **61**, 10322 (2000)
11. Madelung, O., Landolt-Börnstein (eds.): *Semiconductors: Intrinsic Properties of Group IV Elements and III-V, II-VI and I-VII Compounds. New Series, Group III/22a*. Springer, Berlin (1987)
12. Kubis, T., Yeh, C., Vogl, P.: Quantum theory of transport and optical gain in quantum cascade lasers. *Phys. Stat. Sol. (C)* (in press)
13. Vitiello, M.S., Scamarcio, G., Spagnolo, V., Losco, T., Green, R.P., Tredicucci, A., Beere, H.E., Ritchie, D.A.: Electron-lattice coupling in bound-to-continuum THz quantum-cascade lasers. *Appl. Phys. Lett.* **88**, 241109 (2006)